Ikonen, Erkki

Recent advances and perspectives in photometry in the era of LED lighting

Published in:
Measurement Science and Technology

DOI:
10.1088/1361-6501/ad0de6

Published: 01/02/2024

Document Version
Publisher's PDF, also known as Version of record

Please cite the original version:
Ikonen, E. (2024). Recent advances and perspectives in photometry in the era of LED lighting. *Measurement Science and Technology*, *35*(2), Article 021001. https://doi.org/10.1088/1361-6501/ad0de6

Measurement Science and Technology

100 year anniversary
Measurement Science and Technology

PERSPECTIVE • OPEN ACCESS

Recent advances and perspectives in photometry in the era of LED lighting

OPEN ACCESS
IOP Publishing
Measurement Science and Technology
Meas. Sci. Technol. **35** (2024) 021001 (11pp)
https://doi.org/10.1088/1361-6501/ad0de6

Perspective

Recent advances and perspectives in photometry in the era of LED lighting

Erkki Ikonen

Metrology Research Institute, Aalto University, Espoo, Finland
VTT MIKES, VTT Technical Research Centre of Finland Ltd, Espoo, Finland

E-mail: erkki.ikonen@aalto.fi

Received 6 July 2023, revised 4 November 2023
Accepted for publication 17 November 2023
Published 29 November 2023

Abstract

Photometry contributes to our understanding how the world is perceived by the human visual system, where a specific example is an early study of photographic plates. Nowadays photometry has an important role in measurement of lighting, particularly in the transition from incandescent lighting to LED lighting. In the context of sustainability and energy efficiency, updated photometric methods are needed that address the spectral, color, geometrical, and temporal characteristics of LED light sources. Highlights of the recent advances in these measurement methods are reviewed. Furthermore, challenges and achievements are described in the measurement of optical power, particularly related to the definition of the photometric SI base unit, the candela. These achievements are based on progress in the development of underpinning optical measurement standards, with a focus on technologies like the electrical substitution radiometer and the predictable quantum efficient detector. As a conclusion, the importance of ongoing research and development in photometry is emphasized considering its crucial role in supporting the advances of LED lighting technology and sustainable development goals of lighting industry.

Keywords: photometry, light emitting diode, optical power measurements

1. Introduction

Photometry aims to characterize the world around us in the same way as it is sensed by the human visual system. One of the early studies by Bull and Mills Cartwright [1] was measurement of photographic density of negatives, where the brightness matching of a human observer was essential for a reliable result. The needs of printing industry have changed, but the quality of printed and displayed images is still of their utmost importance.

The method used in [1] was similar as employed at the same time for determining the photopic luminous efficiency function [2–5] and later standardized by the International Commission on Illumination (CIE) with a symbol $V(\lambda)$ [6]. Those works are important for the lighting industry contributing to the sustainable development by reducing energy consumption. Sustainable development goals are addressed by transition from incandescent lighting to LED lighting [7, 8] which has brought up new measurement needs and emphasized the significance of reliable photometry for ensuring the high quality of lighting.

As lighting is nowadays based on LEDs, it is appropriate to revise the photometric methods from use of incandescent lamps to those of LED light sources. For example, CIE has recently published a LED Reference Spectrum for Photometer Calibration [9], largely based on research concerning the advantages of LED based calibration sources for photometers used with LED lighting [10]. Future work in photometry may take full advantage of the new reference spectrum and related LED based calibration sources when they start to become widely available.

Many features of lighting change with LEDs, such as spectral, color, geometrical and temporal characteristics. Lighting industry needs reliable measurements on all these features which forms a continuing challenge for research laboratories aiming to develop measurement methods with low uncertainties. Finally, the underpinning scales of optical power measurements are needed to quantify the energy savings gained by LED lighting as compared with earlier types of lighting. It is noteworthy that there has been a simultaneous development of optical power measurements during the past 100 years, which is reflected in the gradually changing definitions of the photometric base unit of the SI system–the candela [11–13].

2. LEDs for lighting

Technologies for artificial lighting have been under significant development. The history of incandescent lighting dates back to the early 19th century when inventors began experimenting with electric light. Thomas Edison's groundbreaking invention revolutionized the way of illuminating homes and cities, gradually replacing gas and oil lamps. Following the prolonged dominance of incandescent lighting throughout much of the 20th century, the growing demand for environmentally sustainable and economically viable alternatives prompted the emergence of new lighting technologies. Compact fluorescent lamps gained popularity as an energy-efficient replacement for incandescent bulbs [8]. These lamps utilized a combination of gas and phosphors to produce light, offering significant energy savings. Additionally, halogen bulbs were introduced, providing improved efficiency and longer lifespans compared to traditional incandescent bulbs. These developments marked a transition towards more sustainable lighting options, laying the groundwork for further advancements in lighting technology and the eventual rise of even more efficient alternatives.

The true breakthrough came with the advent of LED technology [14]. LED lighting offers exceptional energy efficiency, long lifespan, and versatile design possibilities. Rapid advancements in LED technology have resulted in increased brightness, improved color accuracy, and reduced costs, making it the preferred choice for residential, commercial, and outdoor lighting applications today. LED lighting has revolutionized the lighting industry, leading in many cases to adapted measurement and characterization methods as compared with those of traditional incandescent lighting.

2.1. Spectral characteristics

LED light sources offer unique spectral characteristics that distinguish them from other lighting technologies. One key aspect is their ability to emit incoherent light in a narrow range of wavelengths, resulting in a more specific color output. With fluorescent materials, LEDs can be engineered to emit light across the whole visible spectrum. Moreover, LED light sources have exceptional color consistency and accuracy, providing a high color rendering index (see appendix for further details) and enabling accurate representation of objects' true colors [15]. The spectral control makes LED light sources ideal for various applications, including lighting design, photography, and horticulture.

In all these applications it is important to quantify the useful amount of light obtained from the LED light sources. Photometers measure light weighted by the $V(\lambda)$ function corresponding to the sensitivity of human eye (see appendix for further details). Photometer responsivities have been traditionally calibrated by observing their signal from a known light source whose spectrum resembles CIE Standard Illuminant A [16], a Planckian radiator at the temperature of 2856.5 K. This method works well with measurements of incandescent lighting, but for LED lighting the spectral mismatch and related uncertainties increase, because the spectral shape of white LEDs is different from Illuminant A.

The photometer calibration for LED lighting applications would improve, if the known light source used for calibration would have a spectrum resembling the usual spectra in LED lighting applications, instead of a spectrum resembling Illuminant A. For this purpose, the spectra of a large number of LED products have been studied and used to calculate representative spectral power distributions (SPDs) for LED sources of different correlated color temperature categories [10]. It was found that in general, when compared with Standard Illuminant A, all potential LED calibration spectra reduced spectral mismatch errors when measuring LED products. The white phosphor-converted LED spectrum with correlated color temperature of about 4100 K was found to be most suitable to complement Illuminant A in luminous responsivity calibrations of photometers. It was used as the basis of spectrum L41 (figure 1), defined as the CIE reference spectrum for photometer calibration [9]. It is noteworthy that a light source resembling L41 works well as a calibration source also with photometers intended for use in daylight applications.

Practical LED light sources [18–20], with spectral irradiance resembling the L41 spectrum, have been developed. Even if their spectra would somewhat deviate from the reference spectrum L41, they would reduce the spectral mismatch error in photometer calibration relative to calibrations using incandescent lamps. The LED light sources [18–20] have also other promising features, such as robustness and stability, which make them attractive as complementary standard lamps, working standards, and comparison artefacts. Their performance will be tested in a forthcoming international comparison measurement with global coverage of participants.

The SPD of a light source determines the emissive tristimulus values, such as X, Y, Z and color coordinates defined as ratios of tristimulus values (see appendix for further details). Spectroradiometers are commonly employed devices that

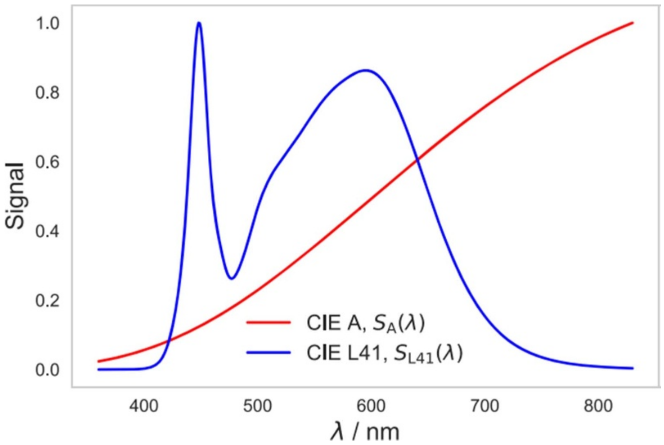

Figure 1. Illuminant A and L41 reference spectrum (Reproduced from [17]. © The Author(s). Published by IOP Publishing Ltd. CC BY 4.0).

analyze the SPD of light emitted by LEDs. To measure color accurately, calibration is crucial [21–26]. Calibration ensures that the measurement results correspond to true spectral shapes across different LED light sources. In addition to spectral analysis, colorimeters are another commonly used tool for color measurement with LEDs. These devices assess color by comparing light intensity across different color filters. Colorimeters offer ease of use and are suitable for various applications such as display calibration and ambient lighting control.

Calibration of spectroradiometers is nowadays based on known incandescent light sources whose spectral irradiance is traceable to black body radiator following Planck radiation law [27–30]. The incandescent working standard lamps are very convenient to transfer the primary calibration from a Planckian radiator to spectroradiometer user. The challenge here is that the use of incandescent lamps for lighting reduces, implying that the availability of incandescent working standard lamps may also reduce. LED light sources designed as new type of working standard are a promising candidate for spectroradiometer calibration in the visible wavelength range, meeting the demands of color measurements. However, research in this area is still at early stages [31, 32] and it is not yet clear that the uncertainties and convenience of use of the earlier incandescent standard lamps are achieved.

Color coordinates are quantities defined in terms of ratios of spectral integrals. They are further used as a basis for calculating other important color quantities. Reliable uncertainty estimation is difficult for ratios of spectral integrals because uncertainty components which are the same at all wavelengths, like aperture area, cancel out and the contribution of noise-like components approaches zero when the number of wavelengths used in the measurement increases. This problem of colour coordinate uncertainty evaluation has been addressed by analyzing partial correlations at neighboring wavelengths through a basis function method [33]. The need for further work in estimating uncertainties of spectral integrals has been recognized [34–36], which is anticipated to yield more reliable uncertainties in colorimetry with LED lighting [37, 38].

2.2. Geometrical characteristics

LED light sources offer directional lighting, with the ability to emit light in specific directions without the need for additional reflectors or diffusers. This directional nature reduces wasted light and enables focused illumination, making LEDs highly efficient for task lighting and spotlighting applications. Furthermore, the small size of LEDs allows for easy integration into different lighting fixtures and applications. LEDs can be designed to emit light in specific directions, resulting in efficient light distribution and reduced light pollution.

The lighting designer needs information on the angular distribution of light intensity, but such information is also essential for measurement purposes. Figure 2 shows examples of angular distributions of LED light sources. Such data are needed when the absolute integrating-sphere method is used for luminous flux measurements of LED lamps [39–42]. Integrating spheres are also widely used in industry where their calibration is traceable to transfer standard lamps or more advanced artifacts [43]. In goniometric setups for luminous flux measurements, the detector or spectroradiometer is moved at known angles relative to the light source [44, 45]. This motion is necessarily slow and such measurements of angular distributions take a long time. An alternative, fast way of obtaining the angular intensity distribution is that the light source illuminates a Lambertian reflecting screen at a large distance and the screen is imaged by a camera [46–48]. Knowing the geometric relation between the system components, it is possible to calculate the intensity distribution within the angular range of the screen or construct the full intensity distribution by rotating a light source with wide angular pattern. The extreme case of this method is to use a 2π camera (fisheye) on the wall aperture of an integrating sphere [49].

The fisheye method was originally developed for spatial non-uniformity corrections in luminous flux measurements with integrating spheres, but it can be also used for fast measurement of light source angular distributions [42, 49]. The method needs to be calibrated for the angular responsivity of the sphere with a light source of known angular distribution,

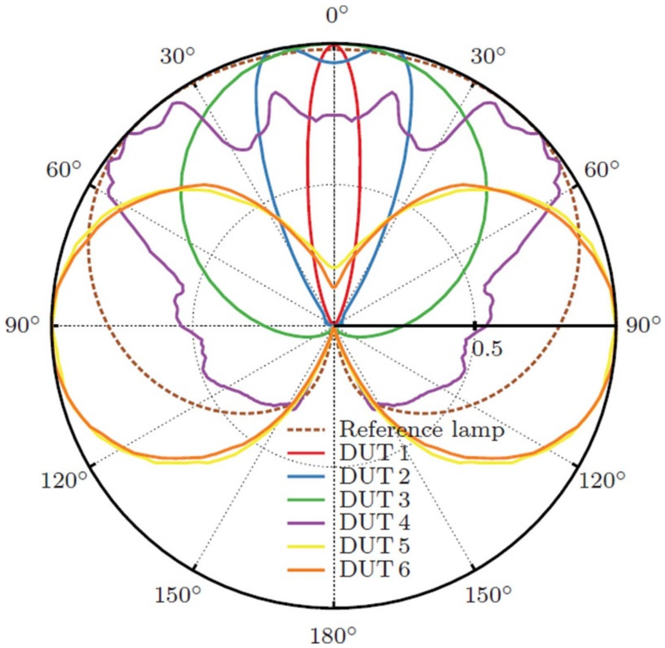

Figure 2. Angular distributions of LED emission intensity [42]. Reproduced from [42].

determined by the goniometric measurement (see figure 3). However, it may be possible to make the fisheye method independent of the goniometric measurements by using a narrow-beam light source in the middle of the sphere [39, 50] and raster-scanning the sphere responsivity in all directions, in a similar way as has been done in accurate optical aperture area measurements [51]. Furthermore, if a 2π hyperspectral camera is used in the sphere wall aperture, combined angular and spectral information may be obtained with the fisheye method.

2.3. Temporal characteristics

The lifetime of LED lamps is very long as compared with alternative technologies, making a significant contribution to sustainability, in addition to energy efficiency. Natural aging monitoring on a time scale of many years is challenging and may lead to intolerable delay in obtaining the results. However, ageing of LED light sources can be accelerated by increasing the junction temperature of the LEDs [52–56]. In extending the LED lamp lifetime, care should be taken to ensure that the driver electronics is not the limiting factor. It has also been found that LEDs operating at higher junction temperatures are more often damaged [57].

LED lights have instant on/off capabilities, providing immediate illumination without any warm-up time. This feature is particularly beneficial in applications where instant lighting is required, such as security lighting or emergency situations. LEDs also excel in dimming capabilities, offering smooth and flicker-free dimming across a wide range of light levels. The LED lamps are quite resistant to frequent switching, ensuring consistent performance and reliability over time. In fact, the first definite observation of reduced lifetime due to switching was observed only recently in natural ageing conditions [58].

Significant energy and cost savings can be obtained with LED lighting when light is used only when needed in buildings, pedestrian areas, and streets [59–61]. Figure 4 shows a comparison of streetlamp ageing results, when one lamp group has natural ageing while another cycled group of lamps has been switched between 20% and 100% power with 30 s interval [58]. Although after 10 000 h of ageing the cycled group shows a few percent lower luminous flux, the switching frequency is about ten times the average switching frequency which would occur in real traffic conditions with smart lighting. Thus, the effect of smart control in energy savings exceeds the increase of maintenance costs due to the decreased lifetime of switched streetlamps [58].

Certain LED lighting installations may exhibit visually harmful temporal effects [62]. In some cases, LEDs operating with poor driver circuitry can cause perceptible flicker, leading to eye strain, headaches, and discomfort. Rapid on/off switching or irregular pulse-width modulation can result in noticeable strobing, which can be distracting and disrupt visual perception. Addressing these issues through proper design, high-quality components, and adequate measurements is crucial to minimize visually harmful temporal effects and ensure a comfortable and visually pleasing lighting experience.

Figure 5 shows examples of light waveforms with different types of LED driver electronics. The new EU Ecodesign regulation set requirements for lighting equipment on the European market starting September 2021. This regulation defined restrictions for two temporal light artefact (TLA) metrics, short-term flicker severity index ($P_{\mathrm{st}}^{\mathrm{LM}}$) and stroboscopic visibility measure (M_{VS}): $P_{\mathrm{st}}^{\mathrm{LM}} < 1$ and $M_{\mathrm{VS}} < 0.4$, to limit TLA effects. For both metrics, the value 1 means that an

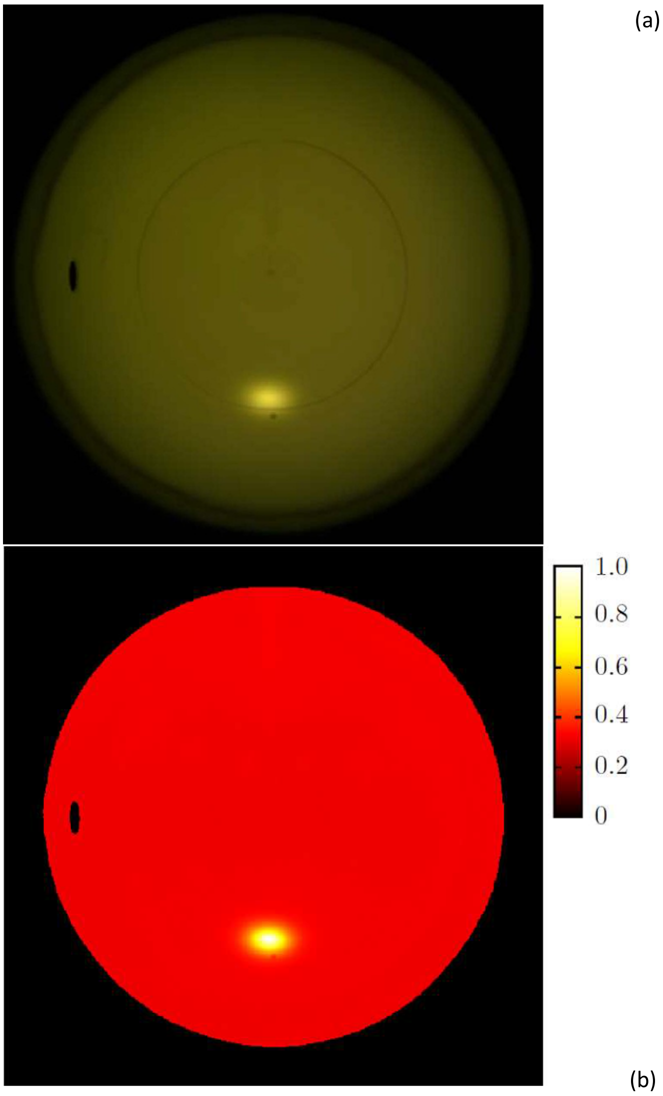

Figure 3. (a) Photograph captured by the fisheye camera inside an integrating sphere with spotlight LED source. (b) Processed photograph for determining the angular intensity distribution of the LED light source. For image processing, a reference photograph is needed where the sphere is illuminated by a light source with an angular intensity distribution as uniform as possible. The seam between the sphere halves, the lamp holder socket at the bottom, and the baffle in the center are visible in (a), but removed in the processed image (b) [49]. (a) and (b) Reproduced from [49].

average observer has 50% chance to perceive these TLAs. When these values are less than one, they are not visible on the average. Measurement methods for the above parameters with LED lighting have been improved recently [63–66].

By comparing the TLA results obtained from the older (before 2017) and newer (after 2021) LED lamps, it can be concluded that the luminaire manufacturers have taken the EU Ecodesign regulation into account. This has been done by favoring better LED driver types, which in general results in lower P_{st}^{LM} and M_{VS} values [67].

3. Underpinning optical measurement standards

Energy efficiency of LED light sources is one of their key advantages. Quantitative determination of this characteristics in units of lm W^{-1} requires measurement of the produced luminous flux and electrical input power of the LED lamp. Although measurement of electrical power sounds simple, the variable AC power line impedance may be a considerable challenge in the case of practical LED lighting [68, 69]. However, here we focus on the luminous flux measurements which are closely related to improvements in the definition of the SI base unit candela.

3.1. Definition of the candela

The definition of the candela, the SI unit for luminous intensity, has undergone significant changes over the years. Historically, the candela was defined as the luminous intensity of a specific type of candle flame. In 1930s, developments started in order to define the candela in terms of blackbody radiation at a specific temperature. This line of development resulted in 1967 in the final form of the 'source-based'

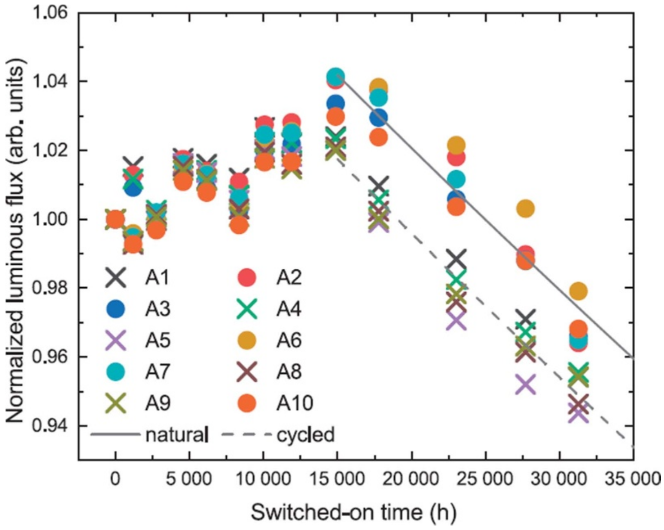

Figure 4. Effect of 30 s cycling between 20% and 100% power on LED streetlamp ageing [58]. Reproduced from [58]. CC BY 4.0.

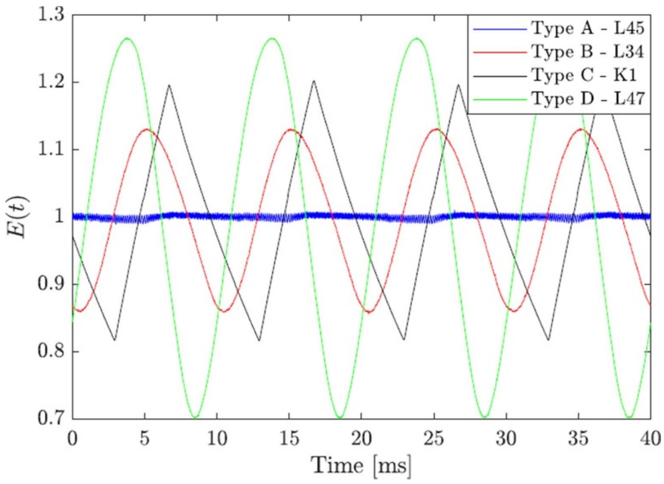

Figure 5. Normalized light waveforms of four LED lamps, each with different driver type A, B, C or D [63]. Reproduced from [63]. CC BY 4.0.

candela where the candela was the luminous intensity, in the perpendicular direction, of a surface of 1 / 600 000 m^2 of a black body at the temperature of freezing platinum under a pressure of 101 325 N m^{-2} [11]. But the difficulties still continued in carrying out easy measurements with this kind of material artifact.

Meanwhile, improved absolute detectors were under development [70, 71] which suggested another approach in the definition of the candela. In 1979, the candela was defined as the luminous intensity in a given direction of a source that emits monochromatic radiation with a frequency of 540 THz and has a radiant intensity of 1/683 watt per steradian [12]. This definition removed the dependence on specific light sources and allowed underpinning optical power measurements for the realization of the definition of the candela [72–74]. The frequency of 540 THz corresponds to a wavelength of 555 nm of optical radiation, which is at the peak of the photopic luminous efficiency function $V(\lambda)$. With light sources containing wavelengths other than 555 nm, the luminous intensity is obtained by weighting with the $V(\lambda)$ function.

In 2019, the SI system underwent a redefinition that further refined the definition of the candela. It is now defined in terms of a fixed numerical value of the luminous efficacy of monochromatic radiation of frequency 540 THz, which is 683 lm W^{-1}, exactly [13]. These changes in the definition of the candela reflect the progress in metrology and the quest for more precise and universal standards in the field of light measurement. Accurate measurement of optical power or detector spectral responsivity continues to be the starting point of traceability for measurement of luminous intensity and luminous flux. The mise-en-pratique for the definition of the candela [13] specifies two detector-based methods as primary standards of optical power: cryogenically cooled electrical substitution radiometer [72–74] and predictable quantum efficient detector (PQED) [75, 76].

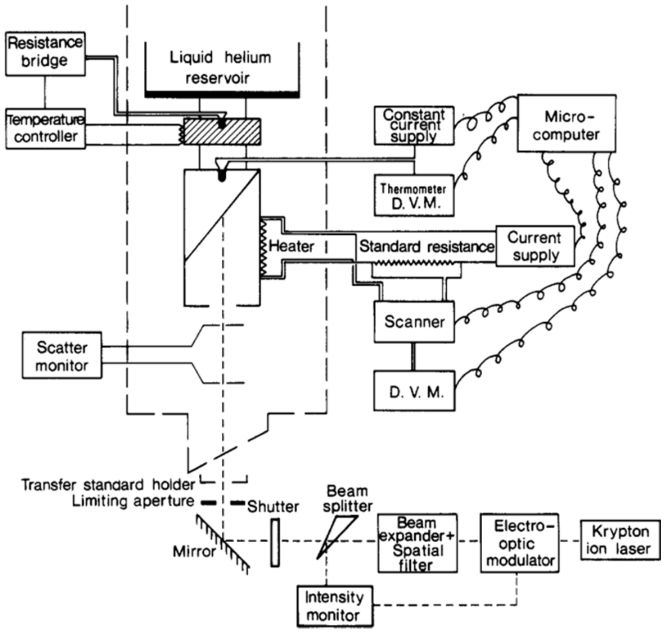

Figure 6. Block diagram of the first cryogenic radiometer for laser power measurement from 1985 [72]. Reproduced from [72].

3.2. Measurement of optical power

The electrical substitution radiometer (ESR) in a cryostat has become the most important optical power standard in metrology laboratories [77], often used with monochromatic laser radiation. The radiation absorber is positioned within the cold cavity of the cryostat at a temperature slightly above the boiling point of helium (figure 6). The cold cavity is alternately heated by electrical wiring and incoming radiation providing traceability of optical power to measured heating current and voltage. Cooling below 10 K significantly enhances the heat diffusivity of copper, allowing large-size absorption cavity and effectively reducing the non-equivalency between optical and electrical heating [72]. Furthermore, superconducting current leads to the heating wires of the cavity reduce parasitic heating [73]. The ESRs operated at cryogenic temperatures [72–74] thus have significant advantages as compared with room-temperature ESRs [70]. The former devices, capable of measuring absolute optical power with a relative uncertainty of 0.01% or below, are commonly referred to as absolute cryogenic radiometers (ACRs).

An alternative to ACRs is provided by absolute detectors based on induced-junction silicon photodiodes [78–82], where each incoming photon is converted to an exactly one electron-hole pair. The measured photocurrent accurately quantifies the incoming optical power, provided that the vacuum wavelength of the laser radiation is known and the effects of reflectance, absorption, charge-carrier recombination losses and quantum yield can be eliminated or estimated with a relative uncertainty of 0.01% or below. In the PQED [75, 76, 83], all these conditions can be met at the visible wavelength range and relative measurement uncertainties at least as low as with ACRs can be achieved.

Reflectance losses can be reduced with the wedge trap structure of the PQED photodiodes as shown in figure 7 [84]. Furthermore, the correction due to the remaining reflection out of the PQED is easy to measure or calculate within a relative uncertainty of 0.001% in responsivity when the thicknesses and refractive indices of the SiO_2 coating layers are known [85]. The absorption of SiO_2 at visible wavelengths has been estimated to be negligible [81]. Recently, a method for very accurate determination of the correction due to charge-carrier recombination losses was introduced [86]. The method is based on measurement and analysis of the photocurrent as a function of reverse bias voltage of the PQED photodiodes [87]. Fitting of a 3D simulation model of charge-carrier recombination losses to the photocurrent-voltage data allows to determine the critical parameters of bulk and surface recombination losses. The developed fitting method makes the PQED an independent primary standard of spectral responsivity at the relative uncertainty level of 0.003%. Finally, models have also been developed to account for the effects of quantum yield at short visible wavelengths with sufficient accuracy for the needs of photometry [88, 89].

The PQED photodiodes with SiO_2 coating were originally manufactured from low-doping *p* type silicon [75]. It is also possible to make PQED photodiodes from low-doped *n* type silicon, but then Al_2O_3 has been used as the coating material to produce the induced junction [90, 91]. The charge-carrier recombination losses of *n* type photodiodes appear to be somewhat larger than those of *p* type photodiodes. A new invention of nitride coating on top of a thin SiO_2 layer has been developed for *p* type PQED photodiodes [92]. The performance of the nitride coated photodiodes is at least as good as that of the original *p* type PQED photodiodes [75]. This is an important achievement because

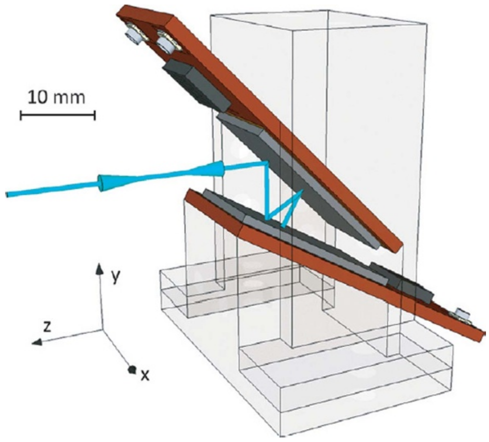

Figure 7. PQED phoatodiodes assembled into a light trap configuration [75]. Reproduced from [75]. © IOP Publishing Ltd All. rights reserved.

it demonstrates that PQED photodiodes with very good characteristics can be produced by professional photodiode manufacturers and thus PQED photodiodes can be made widely available.

Operation of a PQED at room temperature is as easy as operation of Hamamatsu-photodiode-based trap detectors, widely employed as spectral responsivity working standards in photometry. Gas flow through the detector aperture is used to protect the PQED photodiodes from dust in ordinary laboratory room and such protection should actually be used with all accurately calibrated detectors. In irradiance mode measurements, where incident light enters close to the aperture edge, synthetic dry air should be used as flowing gas to avoid formation of a gas lens in front of the aperture [93]. Besides simplicity of use and maintenance, another significant advantage of PQED photodiodes is their stable spectral responsivity over long time periods. Comparison between PQEDs and ACRs did not reveal any change of spectral responsivity within approximately 10 years, including measurements at short visible wavelengths [94].

For direct realization of photometric units, the PQED offers an interesting possibility of determining luminous intensity or illuminance of a white LED light source without the $V(\lambda)$ filter [95], which is often the most problematic component in ordinary photometers. For a LED lamp resembling L41 [9], the main uncertainty component would then come from the relative spectrum of the lamp influencing the spectral mismatch correction factor, where the relative spectral responsivity of the PQED would be known within a relative uncertainty of 0.01% or better. Such a PQED photometer without a physical filter would allow all types of photometric weighting to be taken into account numerically, for example scotopic, mesopic [96–98] or any new photometric weighting function based on cone fundamentals [99].

4. Conclusions and outlook

Photometry continues to be an important field of research. LED lighting offers significant energy-saving possibilities compared to traditional lighting technologies. LEDs consume much less electricity to produce the same level of brightness as incandescent bulbs or fluorescent lamps. This translates to substantial energy savings, reducing electricity bills and environmental impact. Furthermore, LEDs have long lifespans, lasting significantly longer than conventional bulbs. Additionally, LED lighting can be easily integrated with smart lighting controls, allowing for customized scheduling, occupancy sensing, and dimming, maximizing energy efficiency by adapting to specific needs and usage patterns. All these developments of LED lighting should be supported by appropriate measurement methods of photometry, described above for the different characteristics of LED light sources.

The changes in the definition of the photometric base unit-the candela-reflect the developments in photometry and metrology demonstrating the importance of the underpinning optical power measurements. During the past decades it was experienced that parallel development of lighting technology and photometry is a continuous source of interesting research topics and it is expected to be so for the foreseeable future.

Data availability statement

No new data were created or analysed in this study.

Acknowledgments

This work is supported by the Academy of Finland Flagship Programme (PREIN), Photonics Research and Innovation (PREIN), decision Number: 320167.

Appendix

Photometric terms and symbols are explained in this appendix.

Color rendering index

Color rendering index (CRI) serves as a metric to assess a light source's capacity to depict the true colors of objects when compared to a source which is spectrally identical to daylight. Light sources with a high CRI are desirable in color-critical applications. Numerically, a CRI value can reach a maximum of 100, aligning with a source whose spectrum closely resembles that of a black body, like incandescent lamps. In contrast, low-pressure sodium lighting yields a negative CRI, while fluorescent lights typically range from approximately 50 for basic types to about 98 for the best multi-phosphor types. Common white-color LEDs often have a CRI of 80 or higher, while some LEDs can achieve a CRI of up to 98.

Photopic luminous efficiency function V(λ)

Photopic luminous efficiency function $V(\lambda)$ represents the average spectral sensitivity of human visual system in brightly lit conditions. Derived from subjective assessments of which among a pair of variously colored lights appears brighter, it serves to illustrate the relative responsiveness to light of differing wavelengths. It is not an absolute reference to any individual. The values of $V(\lambda)$ function are tabulated by CIE and the function attains a maximum value of 1 at the wavelength of 555 nm and smoothly decreases to zero when decreasing (increasing) the wavelength to 360 nm (830 nm).

Tristimulus values X, Y, Z and color coordinates x, y

Much of quantitative colorimetry is based on tristimulus values X, Y, Z and color coordinates $x = X/(X + Y + Z)$ and $y = Y/(X + Y + Z)$. Emissive tristimulus values are spectral integrals, such as

$$X = \int L_e(\lambda)\bar{x}(\lambda)\,\mathrm{d}\lambda,$$

and corresponding equations for Y and Z. In the above equation, $L_e(\lambda)$ is the spectral radiance and $\bar{x}(\lambda)$ as well as related $\bar{y}(\lambda)$ and $\bar{z}(\lambda)$ are defined CIE standard observers [6]. Function $\bar{y}(\lambda)$ is the same as $V(\lambda)$. Reflective tristimulus values are defined with the aid of sample reflectance and normalization by SPD of the illuminant.

ORCID iD

Erkki Ikonen https://orcid.org/0000-0001-6444-5330

References

[1] Bull A J and Mills Cartwright H 1923 The measurement of photographic density *J. Sci. Instrum.* **1** 74–81
[2] Ives H E 1912 Studies in the photometry of lights of different colours. I. Spectral luminosity curves obtained by the equality of brightness photometer and flicker photometer under similar conditions *Phil. Mag.* **24** 149–88
[3] Coblentz W W and Emerson W B 1918 Relative sensibility of the average eye to light of different colors *Bull. Bur. Stand.* **14** 167–236
[4] Hyde E P, Forsythe W E and Cady F E 1918 The visibility of radiation *Astrophys. J.* **48** 65–88
[5] Gibson K S and Tyndall E P T 1923 Visibility of radiant energy *Sci Pap. Bur. Stand.* **19** 131–91
[6] ISO 11664-1:2019/CIE S 014: 2019 2019 *Colorimetry—Part 1: Standard Colorimetric Observers* (ISO/CIE)
[7] Pimputkar S, Speck J S, Denbaars S P and Nakamura S 2009 Prospects for LED lighting *Nat. Photon.* **3** 180–2
[8] Jacob B 2009 Lamps for improving the energy efficiency of domestic lighting *Light. Res. Technol.* **41** 219–28
[9] CIE 251:2023 2023 *LED Reference Spectrum for Photometer Calibration* (CIE)
[10] Kokka A *et al* 2018 Development of white LED illuminants for colorimetry and recommendation of white LED reference spectrum for photometry *Metrologia* **55** 526–34
[11] CGPM 1967 *13th CGPM Resolution 5, CR* p 104 1968 *Metrologia* **4** 43–44
[12] CGPM 1979 *16th CGPM Resolution 3, CR* p 100 1980 *Metrologia* **16** 56
[13] BIPM 2019 The international system of units (SI Brochure) 9th edn appendix 2 (Sèvres: BIPM) (available at: https://bipm.org/documents/20126/41489685/SI-App2-candela.pdf)
[14] Tsao J Y, Crawford M H, Coltrin M E, Fischer A J, Koleske D D, Subramania G S, Wang G T, Wierer J J and Karlicek R F 2014 Toward smart and ultra-efficient solid-state lighting *Adv. Opt. Mater.* **2** 809–36
[15] Pust P, Schmidt P J and Schnick W 2015 A revolution in lighting *Nat. Mater.* **14** 454–8
[16] ISO/CIE 11664–2:2022(E) 2022 *Colorimetry—Part 2: CIE Standard Illuminats* (CIE)
[17] Krüger U, Ferrero A, Mantela V, Thorseth A, Trampert K, Pellegrino O and Sperling A 2022 Evaluation of different general $V(\lambda)$ mismatch indices of photometers for LED-based light sources in general lighting applications *Metrologia* **59** 065003
[18] Gerloff T *et al* 2019 Luminous intensity comparison based on new standard lamps with LED reference spectrum *Proc. 29th CIE Session* (*Washington*) pp 77–84
[19] Weiqiang Z, Jinyun Y, Hui L, Ying Y and Yandong L 2021 Temperature dependence correction method of LED filament lamp for total luminous flux calibration based on voltage measurement *Metrologia* **58** 045003
[20] Zhao W, Yan J, Liu H, Su Y and Lin Y 2023 Characterization of the LED filament lamp for luminous intensity calibration *Metrologia* **60** 025004
[21] Hwang J, Lee D-H, Park S, Kim Y-W and Park S-N 2009 Measurement uncertainty evaluation for emission color and luminance of displays *Appl. Opt.* **48** 99–105
[22] Wübbeler G, Campos Acosta J and Elster C 2017 Evaluation of uncertainties for CIELAB color coordinates *Color Res. Appl.* **42** 564–70
[23] Zong Y, Brown S W, Johnson B C, Lykke K R and Ohno Y 2006 Simple spectral stray light correction method for array spectroradiometers *Appl. Opt.* **45** 1111–9
[24] Nevas S, Wubbeler G, Sperling A, Elster C and Teuber A 2012 Simultaneous correction of bandpass and stray-light effects in array spectroradiometer data *Metrologia* **49** S43–7
[25] Pulli T, Nevas S, El Gawhary O, van den Berg S, Askola J, Kärhä P, Manoocheri F and Ikonen E 2017 Nonlinearity characterization of array spectroradiometers for the solar UV measurements *Appl. Opt.* **56** 3077–86
[26] Schinke C, Pollex H, Hinken D, Wolf M, Bothe K, Kröger I, Nevas S and Winter S 2020 Calibrating spectrometers for

measurements of the spectral irradiance caused by solar radiation *Metrologia* **57** 065027
[27] Mielenz K D, Saunders R D, Parr A C and Hsia J J 1990 The 1990 NIST scales of thermal radiometry *J. Res. Natl Inst. Stand. Technol.* **95** 621–9
[28] Sapritsky V I 1995 Black-body radiometry *Metrologia* **32** 411–7
[29] White M, Fox N P, Ralph V E and Harrison N J 1995 The characterization of a high-temperature black body as the basis for the NPL spectral-irradiance scale *Metrologia* **32** 431–4
[30] Sperfeld P, Raatz K-H, Nawo B, Moeller W and Metzdorf J 1995 Spectral-irradiance scale based on radiometric black-body temperature measurements *Metrologia* **32** 435–9
[31] Nakazawa Y, Godo K, Niwa K, Zama T, Yamaji Y and Matsuoka S 2020 Establishment of 2π total spectral radiant flux scale with a broadband LED-based transfer standard source *Metrologia* **57** 065024
[32] Nevas S 2023 New calibration standards and methods for radiometry and photometry after phaseout of incandescent lamps *Book of Abstracts, NEWRAD 2023 Conf.* (*Teddington*) pp 66–67
[33] Kärhä P, Vaskuri A, Mäntynen H, Mikkonen N and Ikonen E 2017 Method for estimating effects of unknown correlations in spectral irradiance data on uncertainties of spectrally integrated colorimetric quantities *Metrologia* **54** 524–34
[34] Vaskuri A, Kärhä P, Egli L, Gröbner J and Ikonen E 2018 Uncertainty analysis of total ozone derived from direct solar irradiance spectra in the presence of unknown spectral deviations *Atmos. Meas. Tech.* **11** 3595–610
[35] Schmähling F, Wübbeler G, Krüger U, Ruggaber B, Schmidt F, Taubert R D, Sperling A and Elster C 2018 Uncertainty evaluation and propagation for spectral measurements *Color Res. Appl.* **43** 6–16
[36] Maham K, Kärhä P and Ikonen E 2023 Spectral mismatch uncertainty estimation in solar cell calibration using Monte Carlo simulation *IEEE J. Photovolt.* **13** 899-904
[37] Maham K, Kosonen V, Peltoniemi J, Kärhä P and Ikonen E 2023 Spectral analysis of deviations from key comparison reference values *Metrologia* (https://doi.org/10.1088/1681-7575/ad0c9e)
[38] Rezazadeh Y, Sperling A, Gerloff T, Krüger U, Ferrero A, Campos J, Pellegrino O, Dubard J and Ikonen E Uncertainty of evaluation of spectral mismatch correction factor submitted
[39] Ohno Y 1998 Detector-based luminous-flux calibration using the absolute integrating-sphere method *Metrologia* **35** 473–8
[40] Hovila J, Toivanen P and Ikonen E 2004 Realization of the unit of luminous flux at the HUT using the absolute integrating-sphere method *Metrologia* **41** 407–13
[41] Poikonen T, Pulli T, Vaskuri A, Baumgartner H, Kärhä P and Ikonen E 2012 Luminous efficacy measurement of solid-state lamps *Metrologia* **49** S135–40
[42] Kokka A *et al* 2019 Validation of the fisheye camera method for spatial non-uniformity corrections in luminous flux measurements with integrating spheres *Metrologia* **56** 045002
[43] Sperling A, Meyer M, Pendsa S, Jordan W, Revtova E, Poikonen T, Renoux D and Blattner P 2018 Multiple transfer standard for calibration and characterization of test setups for LED lamps and luminaires in industry *Metrologia* **55** S37–42
[44] Lindemann M and Maass R 2009 Photometry and colorimetry of reference LEDs by using a compact goniophotometer *MAPAN* **24** 143–52
[45] Lindemann M, Maass R and Sauter G 2015 Robot goniophotometry at PTB *Metrologia* **52** 167–94
[46] Bürmen M, Pernus F and Likar B 2006 Automated optical quality inspection of light emitting diodes *Meas. Sci. Technol.* **17** 1372–8
[47] Moreno I and Sun -C-C 2009 Three-dimensional measurement of light-emitting diode radiation pattern: a rapid estimation *Meas. Sci. Technol.* **20** 75306
[48] Katona M, Trampert K, Schwanengel C, Krüger U and Neumann C 2022 Geometric system analysis of ILMD-based LID measurement systems using Monte-Carlo simulation *J. Phys.: Conf. Ser.* **2149** 012015
[49] Kokka A, Pulli T, Poikonen T, Askola J and Ikonen E 2017 Fisheye camera method for spatial non-uniformity corrections in luminous flux measurements with integrating spheres *Metrologia* **54** 577–83
[50] Lahti K, Hovila J, Toivanen P, Vahala E, Tittonen I and Ikonen E 2000 Realization of the luminous flux unit using an LED scanner for the absolute integrating-sphere method *Metrologia* **37** 595–8
[51] Lassila A, Toivanen P and Ikonen E 1997 An optical method for direct determination of the radiometric aperture area at high accuracy *Meas. Sci. Technol.* **8** 973–7
[52] Wang F-K and Chu T-P 2012 Lifetime predictions of LED-based light bars by accelerated degradation test *Microelectron. Reliab.* **52** 1332–6
[53] Fan J, Yung K-C and Pecht M 2012 Lifetime estimation of high-power white LED using degradation data-driven method *IEEE Trans. Device Mater. Reliab.* **12** 470–7
[54] Baumgartner H, Renoux D, Kärhä P, Poikonen T, Pulli T and Ikonen E 2016 Natural and accelerated ageing of LED lamps *Light. Res. Technol.* **48** 930–42
[55] Padmasali A N and Kini S G 2020 Accelerated degradation test investigation for life-time performance analysis of LED luminaires *IEEE Trans. Compon. Packag. Manuf. Technol.* **10** 551–8
[56] Law T K and Lim F 2018 A practical degradation based method to predict long-term moisture incursion and color change in high power LEDs *IEEE Photonics J.* **10** 1–14
[57] Vaskuri A, Kärhä P, Baumgartner H, Kantamaa O, Pulli T, Poikonen T and Ikonen E 2018 Relationships between junction temperature, electroluminescence spectrum and ageing of light-emitting diodes *Metrologia* **55** S86–95
[58] Askola J, Kärhä P, Baumgartner H, Porrasmaa S and Ikonen E 2022 Effect of adaptive control on the LED street luminaire lifetime and on the lifecycle costs of a lighting installation *Light. Res. Technol.* **54** 75–89
[59] Lau S P, Merrett G V, Weddell A S and White N M 2015 A traffic-aware streetlighting scheme for smart cities using autonomous networked sensors *Comput. Electr. Eng.* **45** 192–207
[60] Tähkämö L, Räsänen R S and Halonen L 2016 Life cycle cost comparison of high-pressure sodium and light-emitting diode luminaires in street lighting *Int. J. Life Cycle Assess.* **21** 137–45
[61] Marino F, Leccese F and Pizzuti S 2017 Adaptive street lighting predictive control *Energy Proc.* **111** 790–9
[62] Bullough J, Sweater Hickcox K, Klein T and Narendran N 2011 Effects of flicker characteristics from solid-state lighting on detection, acceptability and comfort *Light. Res. Technol.* **43** 337–48
[63] Nordlund R 2022 Validation for measurement of temporal light artefacts on LED light sources *MSc Thesis* Aalto University
[64] Mantela V, Nordlund R, Askola J, Kärhä P and Ikonen E Digital implementations for determination of temporal light artefacts of LED luminaires *Light. Res. Technol.* (https://doi.org/10.1177/14771535231212404)
[65] Koch R and Zuber R 2022 Anti-aliasing filter effects on sampling frequency and effects of mathematical

implementation *Proc. CIE Symp. on Advances in Measurement of Temporal Light Modulation* (*Athens, Greece*) pp 46–53

[66] Dam-Hansen C, Coyne S, Isoardi G and Ohno Y 2022 Minimising the uncertainties in the calculation of stroboscopic effect visibility measure *Proc. CIE Symp. on Advances in Measurement of Temporal Light Modulation* (*Athens, Greece*) pp 54–62

[67] Ikonen E, Nordlund R, Mantela V, Askola J and Kärhä P 2022 Improvement in the temporal light artefact metrics of commercial LED lamps *Abstracts of the CIE Symp. on Advances in Measurement of Temporal Light Modulation* (*Athens, Greece*) pp 14–15

[68] Poikonen T, Koskinen T, Baumgartner H, Kärhä P and Ikonen E 2014 Adjustable power line impedance emulator for characterization of energy-saving lamps *Proc. NEWRAD 2014 Conf.* (*Espoo, Finland*) pp 348–9

[69] Ohno Y, Gaudemer J, Oh J S, Dubard J, Jeon S and Scholand M 2021 Solid state lighting annex: IC 2017 interlaboratory comparison

[70] Blevin W R and Brown W J 1971 A precise measurement of the Stefan-Boltzmann constant *Metrologia* **7** 15–29

[71] Quinn T J and Martin J E 1985 A radiometric determination of the Stefan-Boltzmann constant and thermodynamic temperatures between −40 °C and +100 °C *Phil. Trans. R. Soc.* **316** 85–181

[72] Martin J E, Fox N P and Key P J 1985 A cryogenic radiometer for absolute radiometric measurements *Metrologia* **21** 147–55

[73] Varpula T, Seppä H and Saari J-M 1989 Optical power calibrator based on a stabilized green He-Ne laser and a cryogenic absolute radiometer *IEEE Trans. Instrum. Meas.* **38** 558–64

[74] Foukal P V, Hoyt C, Kochling H and Miller P 1990 Cryogenic absolute radiometers as laboratory irradiance standards, remote sensing detectors, and pyroheliometers *Appl. Opt.* **29** 988–93

[75] Sildoja M, Manoocheri F, Merimaa M, Ikonen E, Müller I, Werner L, Gran J, Kübarsepp T, Smîd M and Rastello M L 2013 Predictable quantum efficient detector: I. Photodiodes and predicted responsivity *Metrologia* **50** 385–94

[76] Müller I *et al* 2013 Predictable quantum efficient detector: II. Characterization and confirmed responsivity *Metrologia* **50** 395–401

[77] Zwinkels J C, Ikonen E, Fox N P, Ulm G and Rastello M L 2010 Photometry, radiometry and "the candela": evolution in the classical and quantum world *Metrologia* **47** R15–32

[78] Hansen T E 1978 Silicon UV-photodiodes using natural inversion layers *Phys. Scr.* **18** 471–5

[79] Geist J, Liang E and Schaefer A R 1981 Complete collection of minority carriers from the inversion layer in induced junction diodes *J. Appl. Phys.* **52** 4879–81

[80] Zalewski E F and Duda C R 1983 Silicon photodiode device with 100% external quantum efficiency *Appl. Opt.* **22** 2867–73

[81] Geist J, Brida G and Rastello M L 2003 Prospects for improving the accuracy of silicon photodiode self-calibration with custom cryogenic photodiodes *Metrologia* **40** S132–5

[82] Gran J, Kübarsepp T, Sildoja M, Manoocheri F, Ikonen E and Müller I 2012 Simulations of a predictable quantum efficient detector with PC1D *Metrologia* **49** S130–4

[83] Dönsberg T, Sildoja M, Manoocheri F, Merimaa M, Petroff L and Ikonen E 2014 A primary standard of optical power based on induced-junction silicon photodiodes operated at room temperature *Metrologia* **51** 197–202

[84] Sildoja M, Manoocheri F and Ikonen E 2009 Reflectance calculations for a predictable quantum efficient detector *Metrologia* **46** S151–4

[85] Sildoja M, Dönsberg T, Mäntynen H, Merimaa M, Manoocheri F and Ikonen E 2014 Use of the predictable quantum efficient detector with light sources of uncontrolled state of polarization *Meas. Sci. Technol.* **25** 015203

[86] Tran T, Porrovecchio G, Smid M, Ikonen E, Dönsberg T and Gran J 2022 Determination of the responsivity of predictable quantum efficient detector over a wide spectral range based on a 3D model of charge carrier recombination losses *Metrologia* **59** 045012

[87] Korpusenko M, Manoocheri F, Kilpi O-P, Varpula A, Kainlauri M, Vehmas T, Prunnila M and Ikonen E 2022 Characterization of predictable quantum efficient detector at 488 nm and 785 nm wavelengths with an order of magnitude change of incident optical power *Meas. Sci. Technol.* **33** 015206

[88] Korpusenko M, Vaskuri A, Manoocheri F and Ikonen E 2023 Impact ionization in silicon at low charge-carrier energies *AIP Adv.* **13** 085119

[89] Korpusenko M, Vaskuri A, Manoocheri F and Ikonen E 2023 Internal quantum efficiency of silicon photodetectors at ultraviolet wavelengths *Metrologia* **60** 055010

[90] Dönsberg T *et al* 2017 Predictable quantum efficient detector based on n-type silicon photodiodes *Metrologia* **54** 821–36

[91] Tanabe M, Shitomi H, Dönsberg T and Ikonen E 2021 Characterization of predictable quantum efficient detector in terms of optical non-linearity in the visible to near-infrared range *Metrologia* **58** 055012

[92] Koybasi O *et al* 2021 High performance predictable quantum efficient detector based on induced-junction photodiodes passivated with SiO_2/SiN_x *Sensors* **21** 7807

[93] Askola J, Maham K, Kärhä P and Ikonen E 2021 Increased detector response in optical overfilled measurements due to gas lens formation by nitrogen flow through the entrance aperture *Metrologia* **58** 055008

[94] Porrovecchio G, Linke U, Smid M, Gran J, Ikonen E and Werner L 2022 Long-term spectral responsivity stability of predictable quantum efficient detectors *Metrologia* **59** 065008

[95] Pulli T, Dönsberg T, Poikonen T, Manoocheri F, Kärhä P and Ikonen E 2015 Advantages of white LED lamps and new detector technology in photometry *Light* **4** e332

[96] CIE 191:2010 2010 *Recommended System for Mesopic Photometry Based on Visual performance* (CIE)

[97] Shpak M, Kärhä P, Porrovecchio G, Smid M and Ikonen E 2014 Luminance meter for photopic and scotopic measurements in the mesopic range *Meas. Sci. Technol.* **25** 095001

[98] Shpak M, Kärhä P and Ikonen E 2017 Mathematical limitations of the CIE mesopic photometry system *Light. Res. Technol.* **49** 111–21

[99] Stockman A and Sharpe L T 2000 The spectral sensitivities of the middle- and long-wavelength-sensitive cones derived from measurements in observers of known genotype *Vis. Res.* **40** 1711–37